Cellulose (2022) 29:3529–3544
https://doi.org/10.1007/s10570-022-04477-x

ORIGINAL RESEARCH

Recyclable, superhydrophobic and effective Ag/TiO_2@PDMS coated cotton fabric with visible-light photocatalyst for efficient water purification

Meiling Zhang · Shuai Jiang · Fuyi Han · Heping Chen · Ni Wang · Liying Liu · Lifang Liu

Received: 18 October 2021 / Accepted: 8 February 2022 / Published online: 26 February 2022

Abstract Multifunctional materials for water purification have attracted significant attention due to the increased water pollution problems. However, fabricating the low-cost, effective, and recyclable separation material for wastewater containing various hazardous substances is still a challenge. Herein, we developed an Ag/TiO_2@PDMS coated cotton fabric with self-cleaning ability, high flux, superior visible-light photocatalytic ability, and recyclability via the "powder + glue" strategy. The composites are superhydrophobic (water contact angle 157°) and show high separation efficiency. After 20 times of repeated use, the separation efficiency remains 16,322 Lm^{-2} h^{-1}, and methylene blue (MB) 's degradation rate remains almost unchanged. The high oil purification, catalytic property, excellent stability in harsh conditions, and recyclability enable the material as a satisfactory candidate for water purification.

Graphical abstract

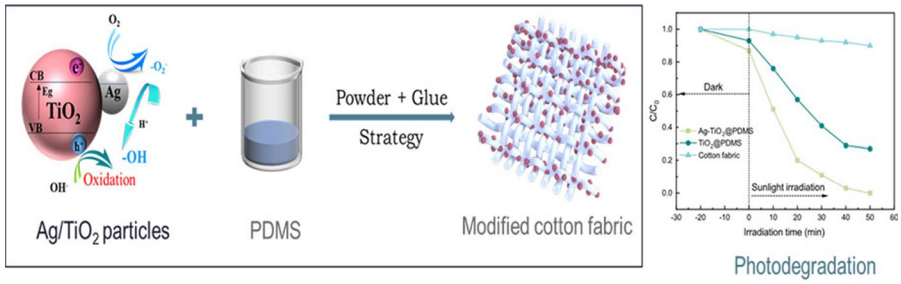

Supplementary Information The online version contains supplementary material available at https://doi.org/10.1007/s10570-022-04477-x.

M. Zhang · S. Jiang · F. Han · H. Chen · N. Wang · L. Liu · L. Liu (✉)
Donghua University, Shanghai, China
e-mail: lifangliu@dhu.edu.cn

Keywords Recyclability · Superhydrophobic cotton fabric · Visible-light photocatalysis · Anti-fouling · Water–oil separation

Introduction

Water pollution, including frequent crude oil leakages and the discharge of organic solvents, has become a severe threat to marine species, human beings, and the ecological environment (Fan et al. 2021). Efficient, selective, economical, and eco-friendly materials for water purification are highly required (Ahmad et al. 2019). Currently, oil/water separation materials with distinct opposite affinities toward water and oil have gained increasing attention (Dong et al. 2019). Materials with special wettability were designed and fabricated by regulating the structure and controlling the material's surface energy (Chen et al. 2019). Inspired by the natural superhydrophobic phenomenon, different kinds of super wetting materials (Su et al. 2016; Ueda and Levkin 2013), including polymer membranes (Jin et al. 2021; Nayak et al. 2021), metallic meshes (Liu and Jiang 2011), textiles (Cao et al. 2016; Chauhan et al. 2019; Cheng et al. 2019; Lin et al. 2019; Yang et al. 2020), and sponge-based 3D absorbents (Chi et al. 2021; Nong et al. 2021; Qu et al. 2021b) were investigated. However, due to the wastewater containing various kinds of oils and water-soluble dyes (Boningari et al. 2018), most of the oil/water separation materials can not satisfy the requirement for effective separation of oil–water emulsion with the micro-nano scale pore sizes (Ma et al. 2020a, 2020b; Yu et al. 2020; Zhan et al. 2020b). Significantly, separation materials are easily contaminated by oily and dye contaminations in the wastewater treatment process, causing secondary pollution to the environment and the high comprehensive cost of post-treatment (Ma et al. 2020b). The poor corrosion resistance, low reusability, as well as a complex and time-consuming fabrication process significantly restricted the practical application of the oil/water separation materials.

Photocatalytic technology uses practical reactive oxygen species to reduce pollutions into harmless low molecular weight molecules and effectively resolve water pollutions (Li et al. 2021; Pan et al. 2020). TiO_2 (Pan et al. 2019), α-Fe_2O_3 (Zheng et al. 2018), ZnO (Lee et al. 2021), CeO_2 (Zhao et al. 2021), $BiVO_3$ (Benaissa et al. 2021), and BiOBr (Liu et al. 2021b) are the most widely used nanoparticle photocatalytic materials. Titanium dioxide (TiO_2), fabricating efficient charge transport pathways, and generating long-lived charges for efficient photocatalysis have been widely applied in the photocatalyst field due to the low-cost, selective preparation process, high stability, non-toxicity, and bactercidal action (Cai et al. 2019; Yu et al. 2021). The photocatalytic activity of anatase type TiO_2 is high (Arumugam et al. 2021; Fotiou et al. 2016; Liu et al. 2021a; Qu et al. 2021a). However, the wide band-gap photocatalysts light absorption is only achieved in the ultraviolet region and the photoelectron-hole pair is easy to recombine, which greatly limits its application. Noble metal doping modification can reduce the recombination probability of photoelectron-hole pair, thus improving the catalytic efficiency of titanium dioxide. Ag ions are characterized by high bactericidal efficiency, and broad antibacterial spectrum and resistance, which can affect the reproduction and growth of microorganisms and lead to their eventual death (Dong et al. 2020).

Herein, we developed an eco-friendly and low-cost method to fabricate recyclable Ag-TiO_2@PDMS coated cotton fabric for oil/water separation and degradation of organic contaminants. By combining the advantages of silver nanoparticles (Ag), we fabricated a heterojunction structured photocatalyst, which changed the light absorption range of TiO_2 and improved photocatalytic performance. Polydimethylsiloxane (PDMS) was introduced as a "glue" that attached the Ag-TiO_2 particles to form a micro – nano structure on the surface of cotton fabric, endowing it with superhydrophobic properties and high photocatalytic activity. The superhydrophobic/superhydrophilic fabric can effectively separate the oil/water mixture and emulsion with high flux and purity. Importantly, large-scale water-soluble organic contaminants are transferred into the photocatalytic activity sites due to the high photocatalytic effect. The separation efficiency of oil/water emulsion is as high as 16,482 Lm^{-2} h^{-1}, the purity of separated oil is 99.98%, and the tensile strength is 74.785 MPa. Moreover, the Ag-TiO_2@PDMS tightly attached cotton fabric is easy to recycle and reuse after sunlight irradiation. Hence, the environmentally friendly, easy accessibility composite with high oil – water separation efficiency and visible-light photocatalytic activity

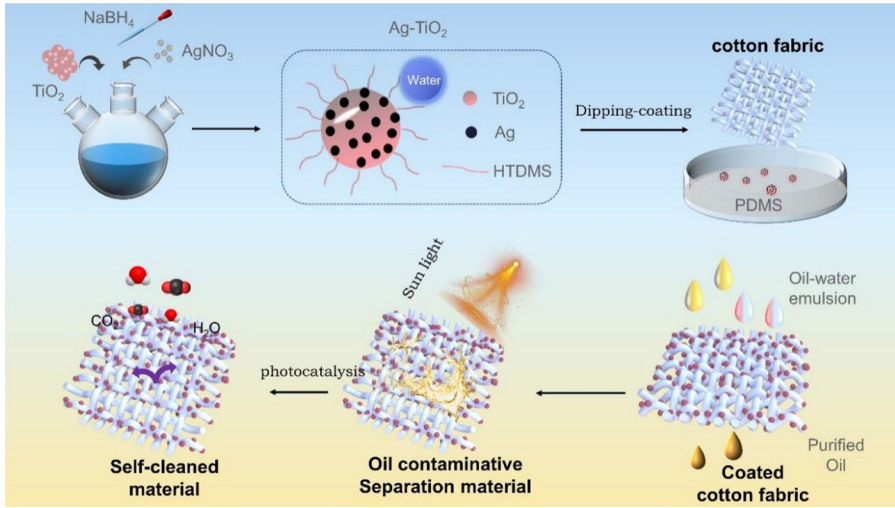

Scheme 1 Preparation process and separation mechanism of Ag-TiO_2@ PDMS coated cotton fabric

provides a novel approach to deal with the water pollution problems.

Experimental section

Materials

Nano titania powder (Titanium(IV) oxide, > 98%, anatase powder), Silver nitrate, cetyltrimethoxy silane (85%), Anhydrous ethanol (99.9%), cyclohexane (99.5%), tetrahydrofuran (99.0%), sodium borohydride (98%), and Methylene blue (95%) were purchased from Shanghai Titan technology co. LTD. Sylgard 184 was obtained from Down Corning.

Preparation of silver decorated TiO_2 (Ag/TiO_2) particles

The modification process of TiO_2 particles and the fabrication schedule of Ag-TiO_2@PDMS coated fabric as illustrated in Scheme 1. TiO_2 (0.2 g) and silver nitrate (5%, 10%, 15%, 20% and 25% of TiO_2 mas ration) were dispersed in distilled water (100 mL) and ultrasonic for 5 min. Then the pH of the solution was adjusted to 10 with ammonia and magnetic stirring for 10 min to get liquid A. To obtain liquid B, the same molar amount of sodium borohydride as silver nitrate was weighed and dissolved in distilled water (10 mL). Then, liquid A and liquid B were mixed and dispersed by ultrasonic for 30 min. The precipitate was collected, cleaned, and then dried overnight in a drying furnace at 50 °C to get Ag- TiO_2 powder. The as-prepared Ag-TiO_2 was dispersed in 50 mL tetrahydrofuran, followed by adding 10 uL, 20 uL, 30 uL, and 40 uL cetyltrimethoxy silane with ultrasonic for 15 min. The fully stirred solution was filtered, and the powder was dried in the oven at 50 °C for 6 h. The prepared samples were named 5% Ag-TiO_2, 10% Ag-TiO_2, 15% Ag-TiO_2, 20% Ag-TiO_2, and 25% Ag-TiO_2 according to the mass ratio of silver nitrate in titanium dioxide.

Preparation of superhydrophobic cotton-based material

The polydimethylsiloxane (PDMS) and curing agent were mixed with the mass ratio of 10:1 and dispersed into 50 mL cyclohexane, and stirred for 30 min. Then, a certain amount of Ag/TiO_2 particles was added to cyclohexane containing PDMS and ultrasonic dispersion for 30 min. The cotton fabric was cut into 6 × 6 cm^2 size and put into Ag-TiO_2/PDMS solution with magnetic stirring for 2 h at 500 rpm. Finally, the soaked fabric was dried at 135 °C for 3 h to obtain the Ag-TiO_2@PDMS coated cotton fabric.

Characterization

The micro morphologies and structure of the as-prepared coated fabric were observed by scanning electron microscopy (SEM, JEOL SU8010) and transmission electron microscopy (TEM, Tecnai F20, Japan), and atomic force microscopy (AFM, Bruker edge). Chemical compositions of the composites were

measured by energy dispersive spectra (EDS, Kevex), Fourier transforms infrared spectra (FT-IR, Nexus 670), and X-ray photoelectron spectra (XPS, Thermo ESCALAB 250XI) and X-ray diffraction (XRD). Thermogravimeter (Diamond TG/DTA, PerkinElmer) was used to test the thermal stability by heating from 30 to 800 °C at a heating rate of 10 °C/min in an N_2 atmosphere. The water contact angles (WCAs) were measured with a contact angle meter (OCA40 Micro, Data Physics, Germany). The feed and filtrate droplet sizes were tested by a dynamic laser scattering (DLS) analyzer measured (Malvern Zeta ZS). The ultraviolet–visible spectroscope (UV–vis, UV-2550) was used to assess the Methylene blue (MB) concentrations in the feed and filtrate.

Water-in-oil immiscible emulsion separation

The Span 80, deionized (DI) water and oil were mixed at the weight ratio of 1:10:100 and vigorously stirred for 6 h. During the water-in-oil emulsion separation experiments, the as-prepared superhydrophobic fabric was fixed inherently between two tubes. The water-in-oil emulsions were poured into the container and permeated through the superhydrophobic coated cotton fabric. After separation, pure oil was flowed down and collected in the bottom vessel. The flux was calculated by calculating the volume of the collected oil within unit time by the following equation:

$$Flux = \frac{V}{A_t}$$

where V is the volume of collected emulsion permeated through the coated cotton fabric, A is the valid test area of the fabric, and t represents the valid time.

Photocatalytic performance measurements

To evaluate the photocatalytic performance of Ag-TiO_2@PDMS coated cotton fabric, MB was used as the model pollutants probes. Photocatalysts (40 mg) were added into MB dye solution (50 mg/L, 100 mL). The solution was placed in the dark for 30 min to achieve adsorption equilibrium. Then, the photodegradation test was employed using a 300 W Xe lamp (BL-CHI-Xe-300) without any filter (320 − 2500 nm). A series of reaction solutions were collected at 10 min intervals. The percentage of degradation is expressed as C/C_0. Here, C_0 is the initial concentration of the dye solution, and C is the dye concentration obtained each time.

Self-cleaning property and reuse ability

The modified cotton fabric's self-cleaning property was tested by removing the dust and MB particles sprinkled on the cotton fabric using water droplets. For recycle and reuse ability measurement, the coated cotton fabric after oil/water separation was placed in the sunlight for a photocatalytic reaction for 1 h and then again for filtration separation. The recycling performance of the separation material was verified by repeated 20 times of the process. Each analyzed sample was filled back for the next period of irradiation.

Results and discussion

Hydrophobic Ag-TiO_2 particles with the high visible light photocatalytic ability

The morphology and structure of the original TiO_2 particles (Fig. S1) and the hydrophobic 15% Ag-TiO_2 were observed by SEM and TEM imaging. TEM analysis shows that the silver particles in hydrophobic 15% Ag-TiO_2 are uniformly attached to the TiO_2 particles, and both Ag and TiO_2 nanoparticles presented nearly spherical shapes. In addition, the diameter of TiO_2 particles is about 100 nm, while the diameter of silver particles ranges from 5 to 40 nm and mainly concentrates on 20 nm (Fig. 1a). The uniform distribution of silver particles on the surface of TiO_2 reduces the bandgap width of TiO_2, and the recombination rate of photogenerated electron–hole pairs thus improves the photocatalytic activity of the particles (Ibrahim et al. 2020). In HRTEM, the distance of the two adjacent planes corresponding to the (101) plane (d value = 3.52 Å) and Ag nanoparticles were identified the (111) plane (d value = 2.35 Å) (Fig. 1b). The ring electron diffraction patterns are presented in Fig. 1c (Karimi-Maleh et al. 2020). Figure 1d shows the (110), (101), (111), and (211) crystal faces of anatase type TiO_2 are respectively corresponding. In general, the sharp diffraction peak of silver nanoparticles can be found in the XRD diffraction pattern, which indicates that the surface of modified titanium dioxide is deposited with suitable crystalline silver nanoparticles. The FTIR spectrum in Fig. S2 also

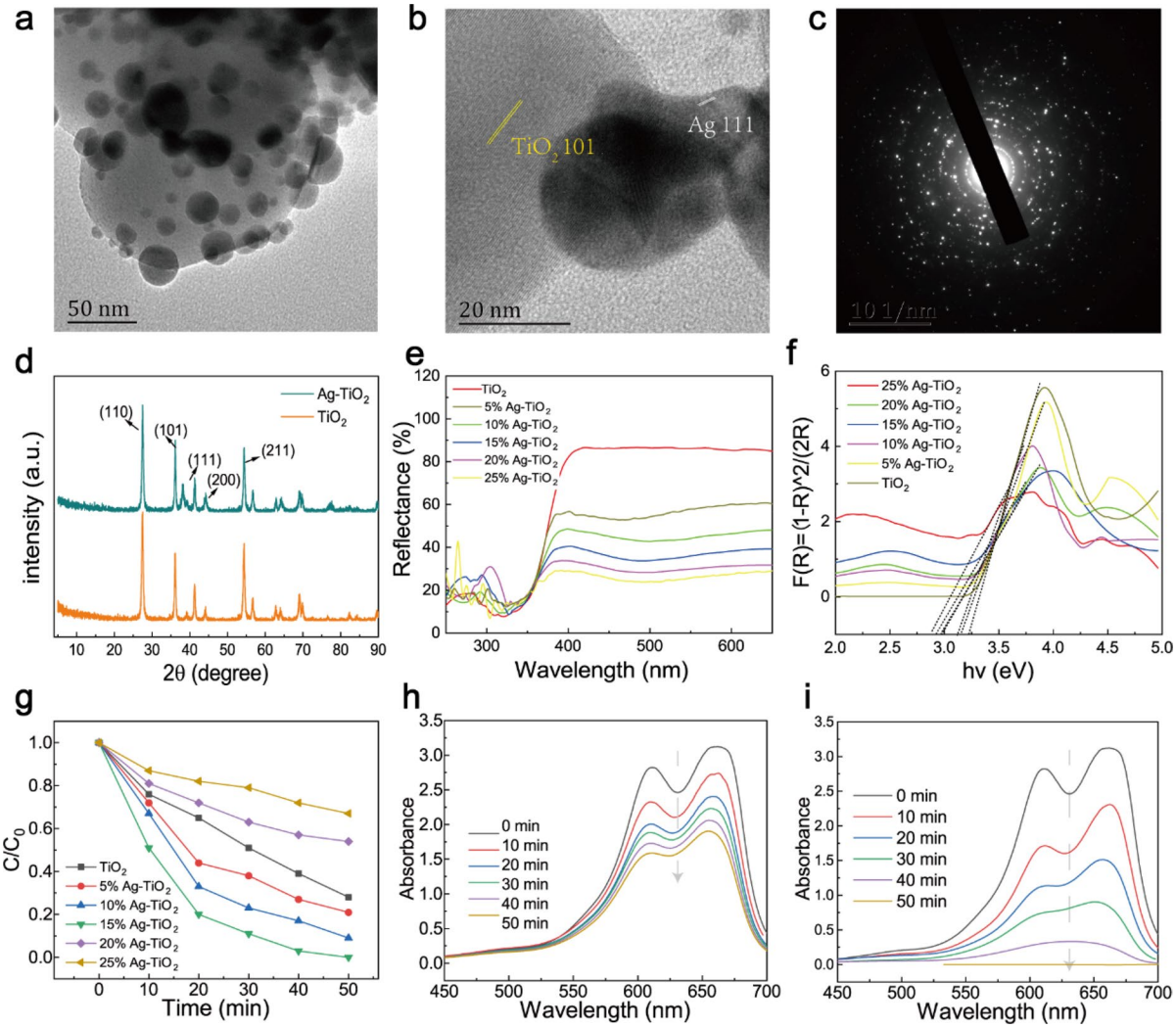

Fig. 1 **A** TEM image of 15% Ag-TiO_2 particles. **b** High-resolution TEM image of Ag-TiO_2 nanocomposites. **c** Electron diffraction pattern of 15% Ag-TiO_2 particles. **d** XRD pattern of TiO_2 and Ag/TiO_2 particles. **e** UV light reflectance and **f** band gaps of Ag-TiO_2 particles with various Ag weight ratios (Xu et al. 2021). **g** Photodegradation of MB solution under visible light. MB absorption spectra of **h** TiO_2 and **i** 15% Ag-TiO_2 after photocatalysis from 0 to 50 min under sunlight

confirmed the existence of Ag. The 15% Ag-TiO_2 presents hydrophobic property (CA = 157°), and the water droplets can slide freely, while the TiO_2 particles easy to absorb water (Fig. S3).

UV–vis diffuse reflectance spectra (UV–vis DRS) were used to assess the light absorption property and electronic band structure of pure TiO_2 and Ag-doped TiO_2 particles. As shown in Fig. 1e, a wide and strong redshift of the absorption edge to the visible light (200–800 nm) reflection of Ag-TiO_2 particles was observed. The reason is that the electronic interactions between Ag and TiO_2 lead to good photocatalytic activity of Ag-TiO_2 under visible light (Xu et al. 2021; Yu et al. 2021). The effect of Ag deposition is observed on metal oxides bandgap through the differential reflectance spectroscopy (DRS) surface analysis. The modified metal oxides were absorbed in the visible region, and redshift (higher wavelength) is predicted in the bandgap of the metal oxides (Fig. 1f). It is to be noted that pure metal oxides have a wide bandgap $TiO_2 = 3.2$ eV, but the bandgap of Ag-TiO_2 nanoparticles is identified as 2.78 eV. The

nanocomposite materials showed longer wavelengths due to the SPR phenomenon, indicating the strong interfacial coupling between TiO_2 and the adjoining Ag in the metallic state. The bandgap energy (Eg) was calculated based on the Kubelka–Munk equation and Tauc's plots (Huo et al. 2021).

As shown in Fig. 1g, the as-prepared Ag-TiO_2 particles exhibit excellent photocatalytic activities for MB degradation under visible light irradiation. The photocatalytic efficiency increased to 80% as the amount of Ag increased to10%. The 15% Ag-TiO_2 particles show the best photocatalytic activity for visible light photocatalytic tetracycline degradation, which is far superior to commercial TiO_2. However, the photodegradation activity decreased while further increasing the Ag doping. This is because small amounts of Ag-doping increase the specific surface area and decrease the nanoparticle size, providing a higher number of reactive sites for photocatalytic processes. However, a higher Ag content strongly reflected the incident UV beam, decreasing the generation of electron–hole pairs, and leading to a declination of the photocatalytic degradation ability.

The simultaneous photocatalysts experiments of TiO_2 and Ag-TiO_2 particles were carried out in the MB mixture (50 mL) under visible light. As shown in Fig. 1h, there is almost no MB degradation for TiO_2 particles under the irradiation of visible light. After modification, the 15% Ag-TiO_2 particles displayed an enhanced dye degradation activity under sunlight (Fig. 1i). The intensity of the absorption peak at 628 nm for Ag-TiO_2reduced drastically with increasing photocatalytic time and completely disappeared after 50 min of irradiation under UV-light while the degradation rate was 50.4% under visible light, indicating the enhanced photocatalysis properties (Wang et al. 2021; Yan et al. 2020; Yu et al. 2021).

Hydrophobic Ag-TiO_2@PDMS coated cotton fabric

The morphologies of Ag-TiO_2@PDMS coated cotton fabrics obtained under different weight ratios of PDMS to Ag-TiO_2 are shown in Fig. S5, S6. As shown in Fig. 2a rough hierarchical surface was formed via attached the Ag-TiO_2 particles upon cotton fabric through PDMS polymer. The EDX elemental mappings also demonstrated that the C, O, Ag, Ti, and Si elements are uniformly distributed in the prepared Ag-TiO_2@PDMS coated fabric, indicating the successful fabrication of superhydrophobic Ag-TiO_2@PDMS coated fabric (Fig. 2b). The FTIR spectrum of cotton fabric before and after coating modification was shown in Fig. 2c. It is evident that the hydrophobic treated fabric maintains the spectral characteristics of cotton fiber.All three fabrics have characteristic peaks of cotton fiber at 3340 cm^{-1}, 2890 , 1314, and 1020 cm^{-1}, corresponding to the -OH tensile vibration, the C-H contraction vibration, and the C-O contraction vibration in the cotton fabric. The infrared peak strength of the hydrophobically modified fabric at 1100 cm^{-1} is related to the tensile vibration of Si–O in the PDMS contained in the first two hydrophobic modified fabrics. In addition, the infrared spectrum of the hydrophobic 15% Ag-TiO_2 fabric is the same as that of the 15% Ag-TiO_2 fabric because the content of hexadecyl trimethoxy silane is too little. Infrared peaks at 795, 1260, and 2962 cm^{-1} were related to the symmetric contraction of Si–O-Si, the bending vibration of Si–C, and the asymmetric tensile vibration of -CH_3, respectively. The result indicates that PDMS has been successfully arranged on the fiber, and the internal structure of cotton fiber has not been changed.

The chemical compositions and states before and after irradiation were further analyzed by XPS. The elements C, O, Ag, Ti, and Si were detected in the full spectrum of the Ag-TiO_2@PDMS coated cotton fabric while there are no Ti, Ag, and Si elements in the cotton fabric (Fig. 2d). Figure 2e demonstrates that three different carbon chemical environments existed in the C1s spectrum of Ag-TiO_2@PDMS. The binding energies of 284.8 eV, 286.4, and 288.2 eV attributed to the C–C/C=C bond, C-O bonds, and C-O-Ti bonds, respectively. As shown in Fig. 2f, the high-resolution O1s spectrum of the Ag-TiO_2@PDMS coated cotton fabric exhibited two peaks at 530.3 eV and 532.0 eV, assigned to Ti–O bonds and oxygen vacancies, respectively. The Si–O and Si-O-Si bonds indicate the successful attaching of PDMS on the cotton fabric (Fig. S8). Exhibited in Fig. 2g are the two different presence of titania state of Ti2p, divided into the Ti $2p_{3/2}$ for TiO-H at 459.1 eV and Ti $2p_{1/2}$ for TiO_2 with BEs of 464.8 eV, respectively. The Ti $2p_{1/2}$—Ti $2p_{3/2}$ splitting (5.7 eV) is related to the Ti^{4+} oxidation state, implying the existence of Ti–O bonds (Pérez-González and Tomás 2021). The two peaks of the Ag spectrum at 373.58 and 367.68 eV are attributed to Ag $3d_{5/2}$ and Ag $3d_{3/2,}$ respectively (Fig. 2h).

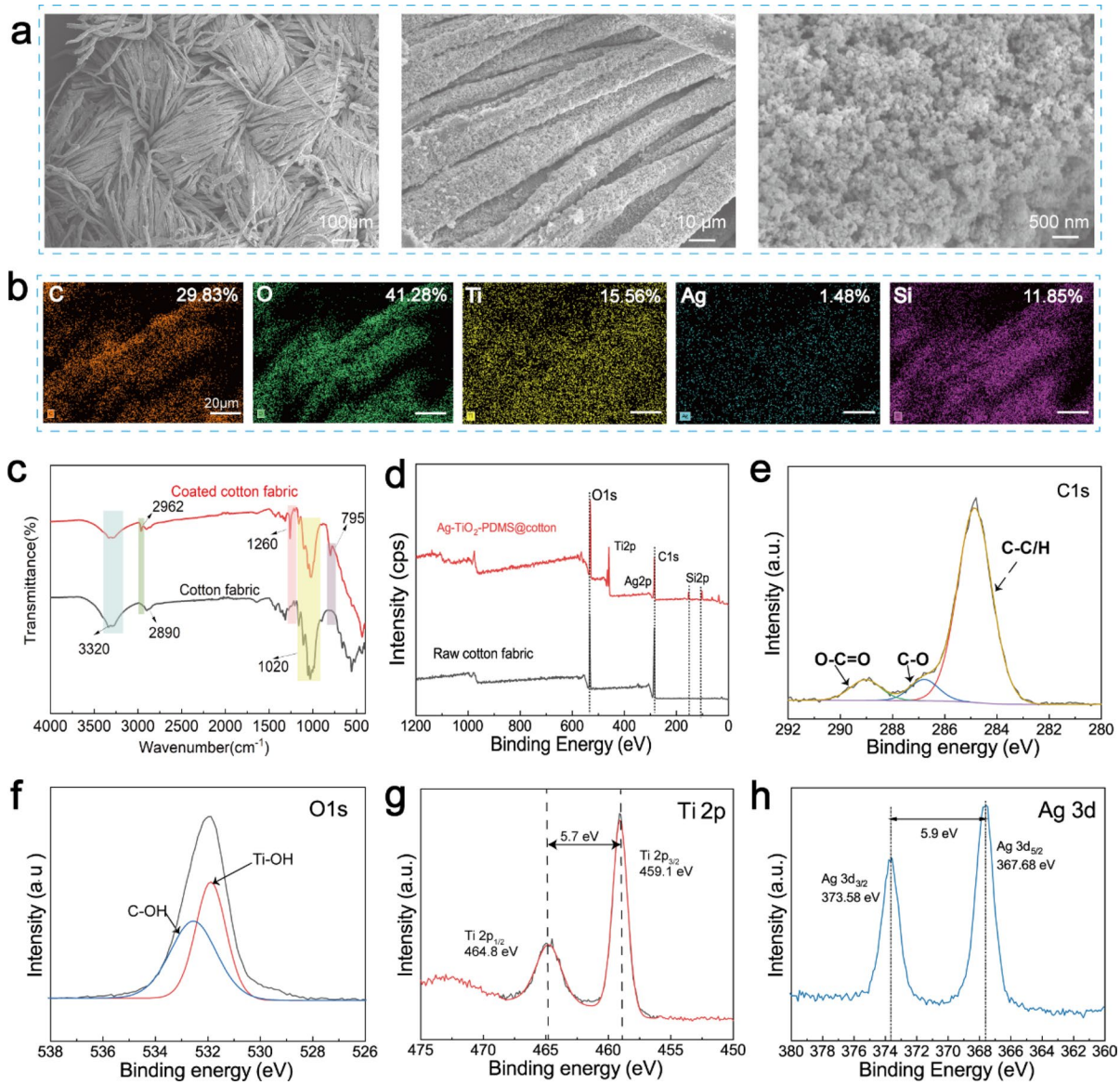

Fig. 2 Macroscopic features and elemental analysis of the microscopic structures of the 15% Ag-TiO_2@PDMS coated fabric. **a** SEM images of the cross-section of 15% Ag-TiO_2@PDMS coated fabric at different degrees of magnification. **b** EDX images of 15% Ag-TiO_2@PDMS coated fabric for the elements C, O, Ti, Ag, and Si, respectively. **c** FTIR spectra, **d** XPS spectrum of cotton fabric and coated fabric. **e** C1s, **f** O1s, **g** Ti2p, and **h** Ag3d spectrums of Ag-TiO_2@PDMS coated fabric

The difference between the two peaks is 6.0 eV, indicating the metallic Ag form. Hence both TiO_2 and Ag existed with their own identity in TiO_2/Ag nanocomposites (Karimi-Maleh et al. 2020; Ma et al. 2020b). The results demonstrated that the PDMS was successfully attached to the surface of the cotton fabric.

Durable hydrophobic and stable mechanical properties

The wettability, determined by the surface structure and chemical composition, is a critical property for wastewater treatment. Figure 3a demonstrated the

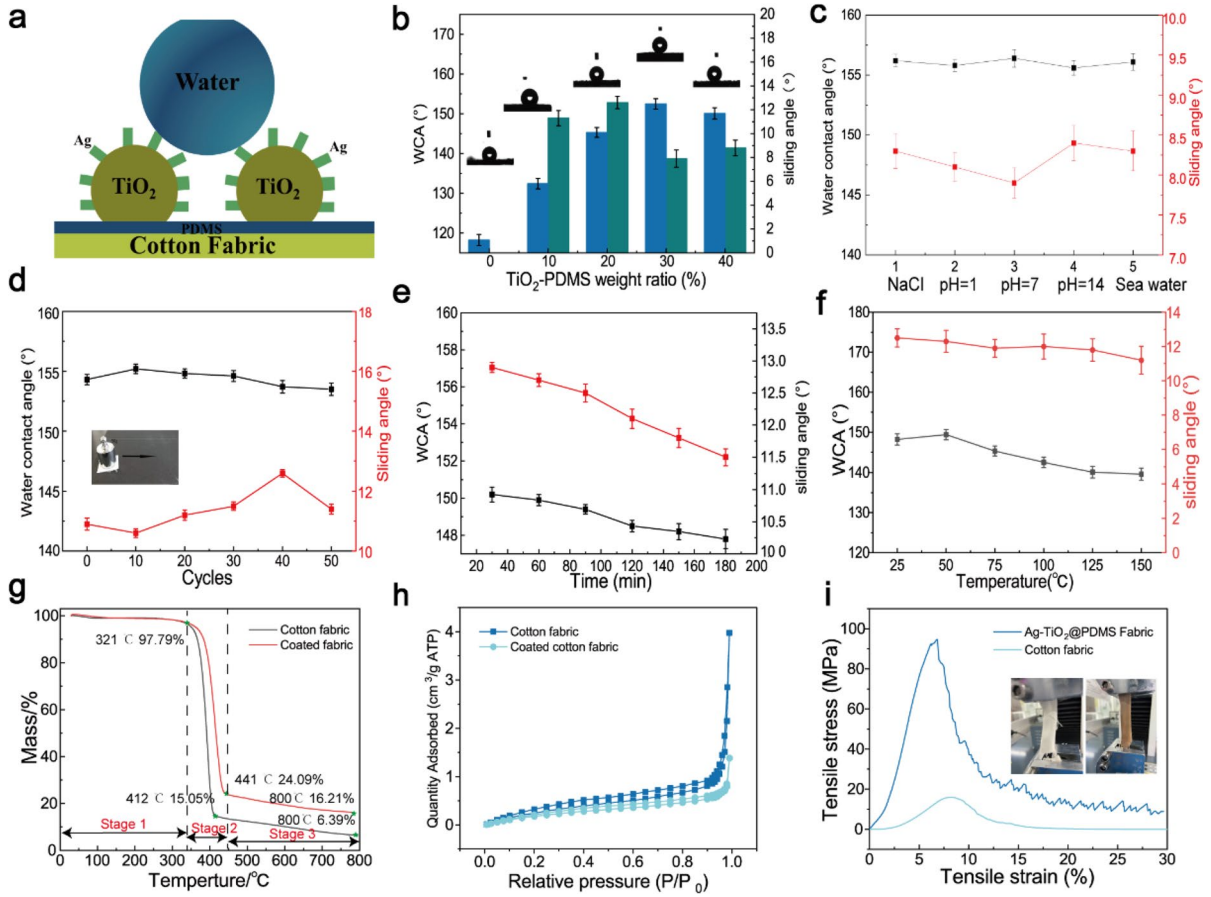

Fig. 3 Wetting behavior of the 15% Ag-TiO_2@PDMS coated fabric and its anti-corrosive ability. **a** Hydrophobic mechanism of Ag-TiO_2@PDMS coated fabric. **b** Contact angles of cotton fabric with various mass ratios of Ag-TiO_2 to PDMS. **c** Water contact angles for solutions with different pH values on the superhydrophobic membranes. **d** Water contact angles under various abrasion cycles. Hydrophobic durability of Ag-TiO_2@PDMS coated fabric under various **e** time and **f** temperatures. **g** Thermogravimetric curve, **h** N_2 adsorption/desorption isotherms (Inset is the pore size curves) of cotton fabric before and after Ag-TiO_2@PDMS coating. **i** Tensile test results of cotton fabric before and after Ag-TiO_2@PDMS coating

superhydrophobic mechanism of coated fabric.The PDMS functioned as a "glue" to embed the Ag-TiO_2 particles on the cotton fabric surface to form superhydrophobic filter materials. The surface roughness of the Ag-TiO_2@PDMS coated fabric was also measured by AFM. The Ag-TiO_2@PDMS coated cotton fabric shows a rough surface in micro-size (Fig. S9). As shown in Fig. 3b, the increase of the mass ratio of Ag-TiO_2 to PDMS leads to a higher water contact angle.

To illustrate the superhydrophobic durability and stability of the Ag-TiO_2@PDMS composite, we investigated the WCAs under harsh conditions, including chemical oxidation, intense light, and physical rubbing. As presented in Fig. 3c, the WCAs of the composite was remained larger than 150° and almost unchanged under different pH, indicating the chemical stability of the coated fabric (Xie et al. 2021; Zhang et al. 2021). The mechanical stability of Ag-TiO_2@PDMS coated fabric was conducted by cyclic abrasion (Chen et al. 2021). As shown in Fig. 3d, after 50 cycles of sliding on a sandpaper substrate (80 grit, 100 g), the WCAs and sliding angles of the modified cotton fabric remained above 150° and below 10°, respectively, indicating the superior stability of hydrophobicity of the modified cotton fabric (Cheng et al. 2020; Yang et al. 2019). Additional testing also evidenced

that the as-prepared Ag-TiO_2@PDMS coated fabric can resist high-temperature treatment and air storage, even after 200 min of air exposure (Fig. 3e) and 150 °C of high-temperature heating (Fig. 3f). As illustrated in Fig. 3g., the Ag-TiO_2@PDMS cotton fabric shown improved thermal stability compared with the pristine cotton fabric. The thermal stability of the Ag-TiO_2@PDMS composite was also confirmed by TG testing. The weight decreased 15.05% for cotton fabric, and 24.09% for coated cotton fabric after the temperature up to 412 °C, and about doubled weight remained for coated fabric compared with pristine cotton fabric at 800 °C (Fig. 3g). The DTG curves (Fig. S10) show that the peak degradation temperature of the cotton fabric is 392.16 °C but shifts to 419.87 °C after coating.

The pore structure and pore size are critical paraments that influence the separation efficiency of the water purification materials. We investigated the pore structure of the cotton fabric and Ag-TiO_2@PDMS coated cotton fabric by using nitrogen adsorption/desorption measurements. As illustrated in Fig. 3h, the nitrogen physisorption isotherm features type-IV behavior, suggesting the coated cotton fabric maintained a hierarchical porous structure (Zhou et al. 2021). The pore sizes are distributed continuously, and the average adsorption pore diameter is 5.1 nm for the cotton fabric and 6.1 nm for coated cotton fabric (Lei et al. 2021). This interconnected hierarchical porous architecture would provide more catalytic sites and improved photocatalytic performance of Ag-TiO_2@PDMS coated cotton fabrics. In addition, the tensile measurement was conducted to study the stretching deformation of Ag-TiO_2@PDMS coated fabric. It is found that the tensile force reaches 74.785 MPa after modification (Fig. 3i).

The separation efficiency of oil/water mixtures and water in oil emulsion

The superhydrophobic/super-oleophilic Ag-TiO_2@PDMS coated cotton fabric has low adhesion to water droplets but selectively allows oil pollution to pass through, leading to a high separation efficiency for oil–water mixtures. A series of oil/water mixtures were applied to evaluate the composite's potential oil/water separation performance for the complex effluents system.

The separation fluxes of Ag-TiO_2@PDMS coated cotton fabric for various oil/water mixtures (Fig. 4a) and water-in-oil emulsions (Fig. 4b) were measured. The results revealed that the modified cotton fabric presents a higher separation flux. For example, the flux of hexane/water mixture and hexane in water emulsion was $14{,}592 \pm 32.1$ and $11{,}397.2 \pm 66.5$ $Lm^{-2}\ h^{-1}$, respectively. Moreover, the oil purity of all coated cotton fabrics was more significant than 99.9% (Jiang et al. 2019). As shown in Fig. 4a, c mixture of dichloromethane and pure water was poured for separation. The dichloromethane quickly passed through the fabric and fell into the container driven by gravity, while the blue water was retained upon the coated cotton fabric. The separation process of the oil/water mixture and the optical microscopy images of feed emulsion and the associated filtrate was shown in Fig. 4d. Numerous micro-scaled water droplets were observed under the optical microscope in the original emulsion while the mixture became transparent after separation and no water droplets were observed, indicating the high separation efficiency of Ag-TiO_2@PDMS coated cotton fabric (Jiang et al. 2019; Zhan et al. 2020a).

Figure 4e presents the emulsion separation procedure of the Ag-TiO_2@PDMS coated cotton fabric. The superhydrophobic property (WCA = 157°) corresponding to a positive ΔP ($\Delta P_w > 0$) renders the coated cotton fabric with excellent water respell ability. In contrast, oil can spontaneously permeate through the Ag-TiO_2@PDMS coated cotton fabric due to the Laplace pressure of the oil being negative ($\Delta P_0 < 0$) (Chen et al. 2019; Gu et al. 2017; Li et al. 2020). Water in the emulsion was filtered out because of the excellent water repellency and size-sieving effect of the Ag-TiO_2@PDMS coated cotton fabric. Contact status between oil and the coating was evaluated as proof of concept. According to the Cassie – Baxter model, the contact status between the liquid and the rough surface can be expressed as:

$$\Delta P = \frac{4\gamma_{SL} cos\theta_{liquid}}{D_{pore}}$$

where ΔP is the Laplace pressure, θ_{liquid} is the WCA of the liquid, and D_{pore} stands for the pore diameter.

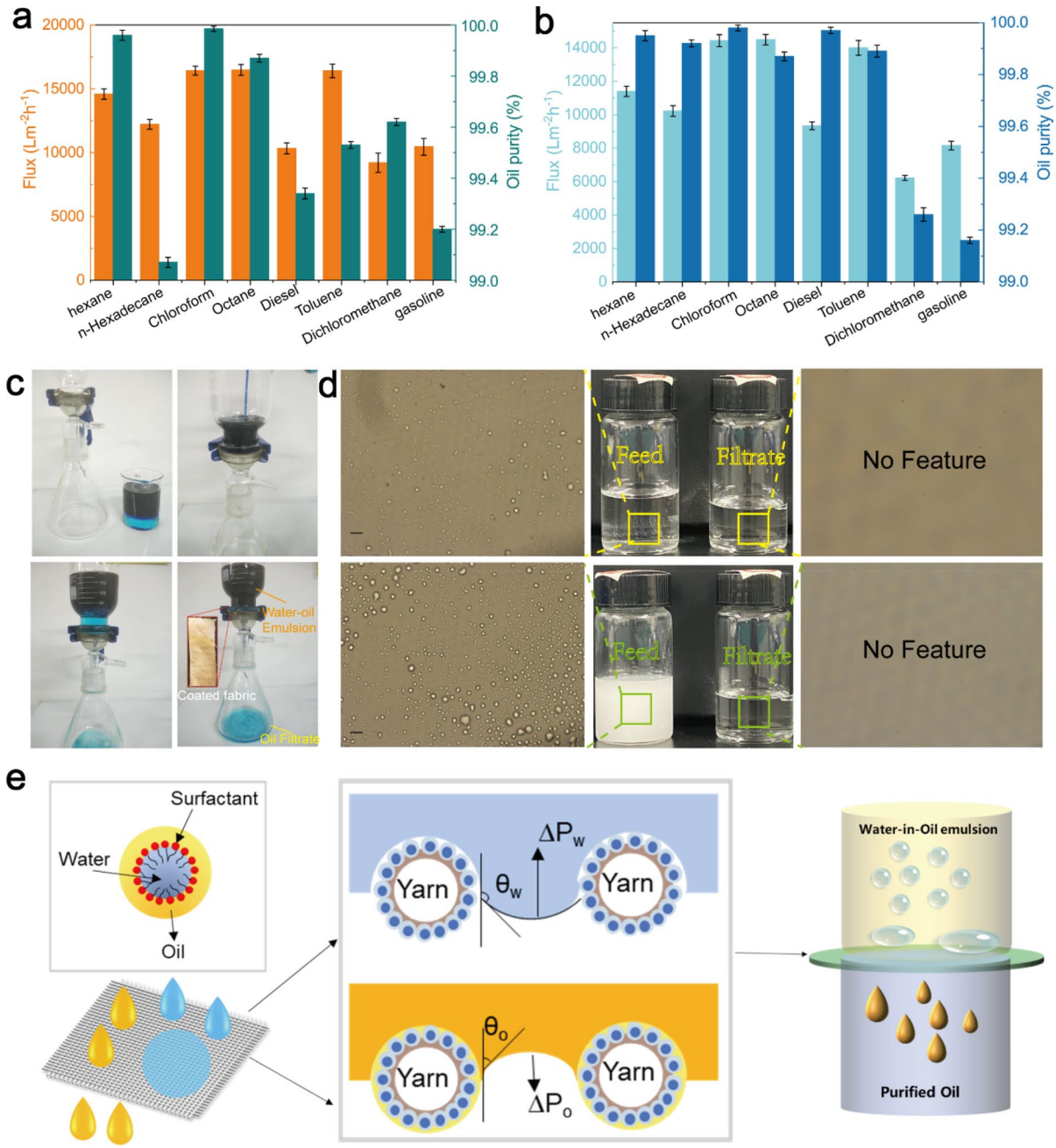

Fig. 4 Separation performance of **a** oil/water mixture and **b** Oil/water emulsion of the resultant coated fabrics. **c** Optical microscope images of oil/water mixture separation by Ag-TiO_2@PDMS cotton fabric: dichloromethane/water mixture separation process and results. Dichloromethane and n-hexane were dyed with methylene blue with 10 mg/ml and 5 mg/ml, respectively. **d** Optical microscope images of the feed and the filtrate of the toluene-in-water emulsion (up) and the acetone-in-water emulsion. Optical microscope images of the emulsions before (left) and after (right) filtration. **e** The hypothetical schematic diagram for separating oil/water mixture and water-in-oil emulsion

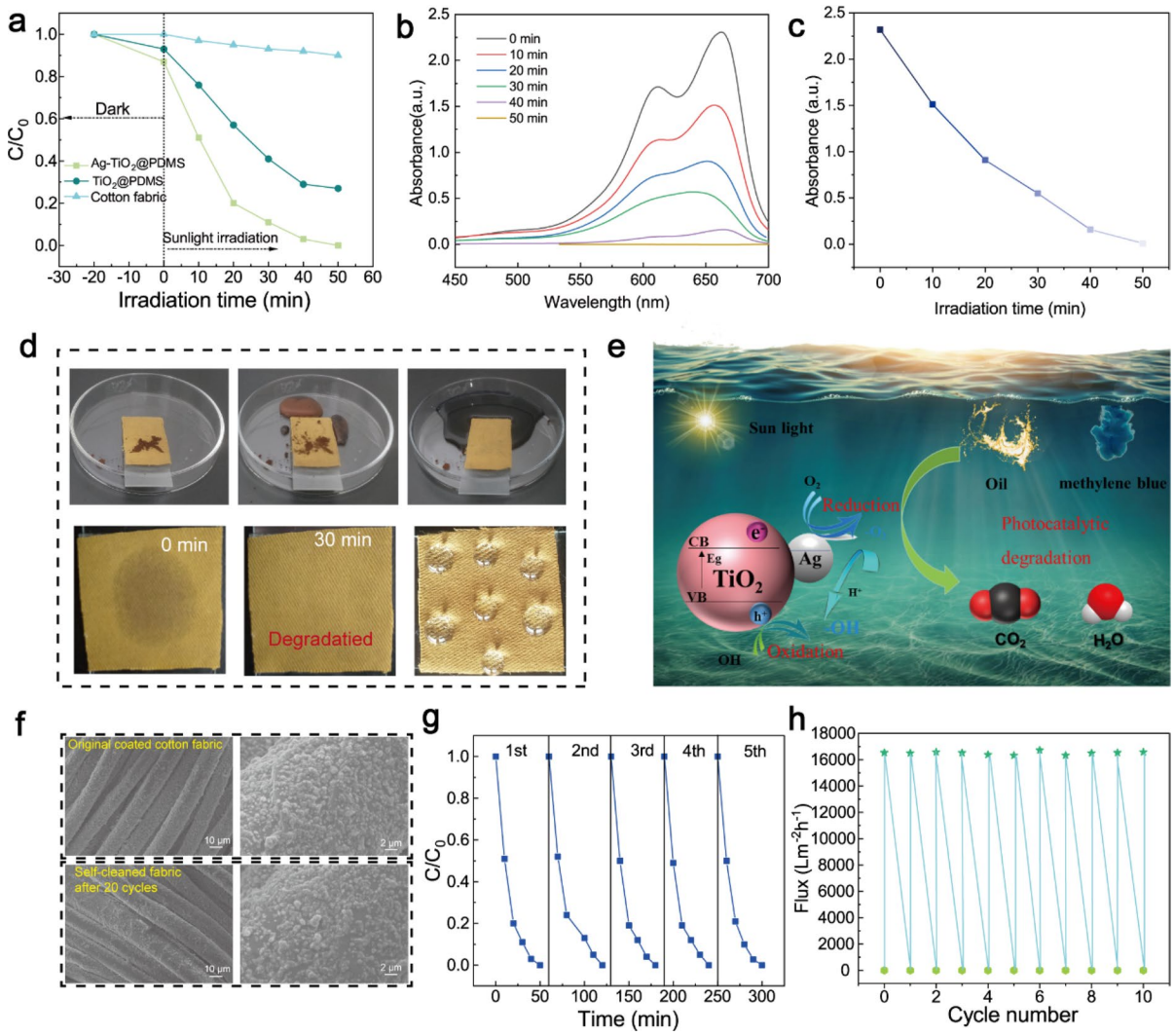

Fig. 5 **a** UV–vis spectrum of MB (C = 8 mg/mL, pH = 5.5) under different time visible light irradiation using Ag-TiO_2@PDMS coated cotton fabric (50 mg). **b** The absorption spectrum of MB solution after photocatalyst degradation by Ag-TiO_2@PDMS coated cotton fabric. **c** Corresponding absorption of MB solution at certain times. **d** Self-clean performance of the coated cotton fabric (up) and photocatalytic efficiency of Ag-TiO_2@PDMS coated cotton fabric (50 mg) (bottom). **e** Photocatalysis mechanism of Ag-TiO_2@PDMS coated cotton fabric for methylene blue and oil. **f** SEM images of the Ag-TiO_2@PDMS coated cotton fabric for the first (up) and 10th cycles (down) after purification. **g** Photocatalytic recycle experiment of Ag-TiO_2@PDMS coated cotton fabric. **h** The separation efficiency of the Ag-TiO_2@PDMS coated cotton fabric for 10 cycles

Photocatalytic ability and recycling performance

Organic dyes are ubiquitous in wastewater, not only posing a challenge in wastewater treatment but causing membrane contamination. We glued the Ag-TiO_2 particles with photocatalysis on cotton fabric by a low-energy PDMS polymer to construct a superhydrophobic surface. Simultaneously, the particles endow the composites with excellent visible light catalytic degradation performance. UV–vis diffuse reflectance spectroscopy (DRS) was used to investigate the optical property of the Ag-TiO_2@PDMS coated cotton fabric, and MB was used as a target organic pollutant to conduct photocatalytic degradation.

As shown in Fig. 5a, the traditional cotton fabric has almost no photocatalytic degradation ability,

while the modified cotton fabric completely degrades MB within about 50 min. Meanwhile, it can be seen that the photocatalytic performance of the modified cotton fabric is better than that of the fabric without Ag modification (70%). The results illustrate that the combination between Ag nanoparticles and TiO_2 can enhance the photocatalytic property under simulated sunlight. The main absorption peak at 464 nm gradually weakened with the increase of irradiation time, indicating the decomposition of MB (Fig. 5b), which is also confirmed by the statistics of the absorption spectrum in Fig. 5c. The enhanced photocatalytic degradation abilities can be explained by the following reasons: 1) the Ag doping upon TiO_2 lowered the band-gap energy, rendering the electrons more easily to transfer from the valence band to the particles conductive band; 2) the Ag-TiO_2 particles broadens the wavelength range, extended adsorption peak from UV-light wavelength to visible light; 3) the porous cotton fabric with Ag-TiO_2 nanoparticles homogenously immobilized, providing more catalytic sites (Zhou et al. 2021).

The pollutants attached to the surface always reduce the photocatalytic activity and separation efficiency of the separation material. Thus, self-cleaning property and reuse ability are critical for water purification materials. Figure 5d shows the anti-pollution performance of the coated cotton fabric (methylene blue and vegetable oil were chosen as the pollutants). The pollutants attached to the surface of the separation materials have been effectively degraded by visible light catalytic degradation of the composite materials prepared in this study, and the recycling of the materials has been realized. No obvious residues remained on Ag-TiO_2@PDMS coated cotton fabric surfaces after recycling, indicating that the Ag-TiO_2@PDMS coated cotton fabric exhibited excellent anti-pollution properties (Cai et al. 2020; Tang et al. 2021).

The photocatalytic degradation mechanism of the Ag-TiO_2@PDMS coated cotton fabric for oil and MB is displayed in Fig. 5e. After irradiation under visible light for 50 min, the MB solution was almost transparent, indicating the excellent photocatalytic activity of the Ag-TiO_2 coated cotton fabric. The Ag-TiO_2 particles attached to the cotton fabric demonstrated a decreasing radius and increasing peak intensities, leading to the strong interaction between MB and the Ag-TiO_2@PDMS coated cotton fabric. When Ag-TiO_2@PDMS coated cotton fabric absorbs optical energy equal to or higher than its bandgap under visible light irradiation, the electrons (e^-) in the valence band (VB) are excited and jumped to the conduction band (CB), generating electron–hole (e^-/h^+) pairs with high activity (Wang et al. 2020). Then, the electron–hole (e^-/h^+) pairs migrated to the surface and reacted with the H_2O and O_2 molecules around it to generate numerous produce superoxide radicals of $\cdot O^{2-}$, reacts with H^+ to form H_2O_2, i.e., hydroxyl (•OH) radicals. The ·OH and $\cdot O^{2-}$ are responsible for oxidizing the oil and MB dye molecules into CO_2 and H_2O, contributing to their high oxidation ability (Yang et al. 2021). From the perspective of environmental protection, the Ag-TiO_2@PDMS coated cotton fabric is a promising candidate for applying wastewater treatment (Ma et al. 2020b).

The recyclability of Ag-TiO_2@PDMS coated cotton fabric is a crucial criterion for the engineering application in the water purification area. The SEM images also illustrated the stability of morphology of Ag-TiO_2@PDMS coated cotton fabric, maintaining the properties of Ag-TiO_2@PDMS coated cotton fabric (Fig. 5f). The reusability of Ag-TiO_2@PDMS coated cotton fabric was evaluated by simultaneous removal of MB in five cycles. The Ag-TiO_2@PDMS coated cotton fabric still exhibits efficient photocatalytic ability after five consecutive cycles (Fig. 5g), indicating promising recyclability. In summary, the Ag-TiO_2@PDMS coated cotton fabric photocatalyst possesses acceptable reusability and stability. As shown in Fig. 5h, ten cycles of the water-in-oil emulsion separation were performed. After each cycle of separation, the filter fabric was subjected to photocatalysis degradation. Though the separation flux decreased slightly, the separation efficiency after separation was maintained above 99% (Lei et al. 2021; Li et al. 2020). As summarized in Table 1, the Ag-TiO_2 coated cotton fabric demonstrated satisfactory separation efficiency, photocatalytic performance, and reuse ability, demonstrating that the as-prepared cotton fabric could be used as a low-cost, effective water purification material with recyclable ability.

Conclusions

In summary, we prepared an effective material for water purification via constructing the micro/nano

Table 1 Comparison of separation efficiency, photocatalytic performance, and reuse ability

Material	Contact angle	SA	Flux $L \cdot m^{-2} \cdot h^{-1}$	Oil purity	Recycle ability	photocatalytic degradation	Ref
MS@TiO_2@PPy Monoliths	165	–	9549	–	8 cycles > 99.5%	94%in 120 min	(Yan et al. 2020)
SCMs (cotton/PVA)	156 ± 2	7.5 ± 1	10,400 ± 400	> 99.9	–	–	(Daksa Ejeta et al. 2020)
SiO_2/PS/PLA	152 ± 2.1	–	8 k–12 k		10 cycles > 90%	–	(Gu et al. 2017)
TiO_2/cotton	> 150	–	36 k–38 k	> 99.5	–	~ 57% in 45 min	(Li et al. 2020)
UIO-66-F4@rGO composites	169.3 ± 0.6°	–	990.45 ± 36.28	–	10 cycles > 99%	–	(Zhan et al. 2020a)
ZIF-8@GSH/PI membrane	130.64–153.25	–	2587.2–5632.9	–	20 cycles > 99/8	91.6%in 120 min	(Ma et al. 2020b)
RGO-PI membrane	–	–	1273.88–2040.04	–	20 cycles	–	(Zhang et al. 2021)
SiO_2/PVDF membrane	130–160	–	16,400 ± 1500	99.95	20 cycles > 99.95%	–	(Wei et al. 2018)
3D melamine sponge	157 ± 2.5	6.2 ± 1.5	–	–	20 cycles > 99.87%	–	(Yang et al. 2019)
rGO@PPS	149.8	–	12,903	99.98	10 cycles > 99.9%	–	(Fan et al. 2021)
Ag/TiO_2@PDMS Composites	157 ± 2.1	10.2 ± 1.5	16,482	99.98	10 cycles > 99.9%;	~ 100%in 50 min	This work

hierarchy surface by immobilizing Ag-TiO_2 and PDMS on cotton fabric. The coated cotton fabric exhibits superhydrophobic properties (WCA = 157°), high flux (16,482 Lm^{-2} h^{-1}), high oil purity up to 99.98%, and exhibits excellent durability in harsh conditions. In addition, the material demonstrated satisfactory photocatalytic activity due to the combination of Ag and TiO_2 reducing the bandgap and enhancing the photocatalytic efficiency under visible-light irradiation. Thus, the material could degrade the organic dyes in the wastewater and be recycled and reused after photocatalysis without performance reduction after 20 cycles. The one-pot process, low cost, high efficiencies, outstanding stability, and can be reused to avoid the environmental pollution and resource waste during the water purification process of the coated cotton fabric, providing a new sight for the advanced materials for large-scale application on water purification area.

Acknowledgments This work was supported by China's National Key R&D Program (Project No. 2018YFC2000900) and Suzhou Science and Technology Project (Project No. ZXL2018134).

Funding The authors have not disclosed any funding.

Declarations

Conflict of interest The authors declare no conflict of interest.

References

Ahmad I, Kan CW, Yao Z (2019) Reactive Blue-25 dye/TiO_2 coated cotton fabrics with self-cleaning and UV blocking properties. Cellulose 26:2821–2832. https://doi.org/10.1007/s10570-019-02279-2

Arumugam V, Kanthapazham R, Zherebtsov DA, Kalimuthu K, Pichaimani P, Muthukaruppan A (2021) Fluorine free TiO_2/cyanate ester coated cotton fabric with low surface free energy and rough surface for durable oil-water separation. Cellulose 28:4847–4863. https://doi.org/10.1007/s10570-021-03822-w

Benaissa M, Abbas N, Al Arni S, Elboughdiri N, Moumen A, Hamdy MS, Abd-Rabboh HSM, Galal AH, Al-Metwaly MG, Ahmed MA (2021) $BiVO_3$/g-C_3N_4 S-scheme heterojunction nanocomposite photocatalyst for hydrogen

production and amaranth dye removal. Opt Mater. https://doi.org/10.1016/j.optmat.2021.111237

Boningari T, Inturi SNR, Suidan M, Smirniotis PG (2018) Novel one-step synthesis of sulfur doped-TiO_2 by flame spray pyrolysis for visible light photocatalytic degradation of acetaldehyde. Chem Eng J 339:249–258. https://doi.org/10.1016/j.cej.2018.01.063

Cai J, Shen J, Zhang X, Ng YH, Huang J, Guo W, Lin C, Lai Y (2019) Light-driven sustainable hydrogen production utilizing TiO_2 nanostructures: a review. Small Methods 3:1800184. https://doi.org/10.1002/smtd.201800184

Cai Y, Chen D, Li N, Xu Q, Li H, He J, Lu J (2020) A self-cleaning heterostructured membrane for efficient oil-in-water emulsion separation with stable flux. Adv Mater 32:2001265. https://doi.org/10.1002/adma.202001265

Cao C, Ge M, Huang J, Li S, Deng S, Zhang S, Chen Z, Zhang K, Al-Deyab SS, Lai Y (2016) Robust fluorine-free superhydrophobic PDMS-ormosil@fabrics for highly effective self-cleaning and efficient oil-water separation. J Mater Chem A 4:12179–12187. https://doi.org/10.1039/c6ta04420d

Chauhan P, Kumar A, Bhushan B (2019) Self-cleaning, stain-resistant and anti-bacterial superhydrophobic cotton fabric prepared by simple immersion technique. J Colloid Interf Sci 535:66–74. https://doi.org/10.1016/j.jcis.2018.09.087

Chen C, Weng D, Mahmood A, Chen S, Wang J (2019) Separation mechanism and construction of surfaces with special wettability for oil/water separation. Acs Appl Mater Inter 11:11006–11027. https://doi.org/10.1021/acsami.9b01293

Chen S, Liu Y, Wang Y, Xu K, Zhang X, Zhong W, Luo G, Xing M (2021) Dual-functional superwettable nanostructured membrane: from ultra-effective separation of oil-water emulsion to seawater desalination. Chem Eng J 411:128042. https://doi.org/10.1016/j.cej.2020.128042

Cheng D, Zhang Y, Bai X, Liu Y, Deng Z, Wu J, Bi S, Ran J, Cai G, Wang X (2020) Mussel-inspired fabrication of superhydrophobic cotton fabric for oil/water separation and visible light photocatalytic. Cellulose 27:5421–5433. https://doi.org/10.1007/s10570-020-03149-y

Cheng Y, Zhu T, Li S, Huang J, Mao J, Yang H, Gao S, Chen Z, Lai Y (2019) A novel strategy for fabricating robust superhydrophobic fabrics by environmentally-friendly enzyme etching. Chem Eng J 355:290–298. https://doi.org/10.1016/j.cej.2018.08.113

Chi H, Xu Z, Wei Z, Zhang T, Wang H, Lin T, Zhao Y (2021) Fabrics with novel air-oil amphibious, spontaneous one-way water-transport capability for oil/water separation. Acs Appl Mater Inter 13:29150–29157. https://doi.org/10.1021/acsami.1c06489

Daksa Ejeta D, Wang CF, Kuo SW, Chen JK, Tsai HC, Hung WS, Hu CC, Lai JY (2020) Preparation of superhydrophobic and superoleophilic cotton-based material for extremely high flux water-in-oil emulsion separation. Chem Eng J 402:126289. https://doi.org/10.1016/j.cej.2020.126289

Dong BB, Wang FH, Yang MY, Yu JL, Hao LY, Xu X, Wang G, Agathopoulos S (2019) Polymer-derived porous SiOC ceramic membranes for efficient oil-water separation and membrane distillation. J Membr Sci 579:111–119. https://doi.org/10.1016/j.memsci.2019.02.066

Dong J, Huang J, Wang A, Biesold-McGee GV, Zhang X, Gao S, Wang S, Lai Y, Lin Z (2020) Vertically-aligned Pt-decorated MoS_2 nanosheets coated on TiO_2 nanotube arrays enable high-efficiency solar-light energy utilization for photocatalysis and self-cleaning SERS devices. Nano Energy 71:104579. https://doi.org/10.1016/j.nanoen.2020.104579

Fan T, Su Y, Fan Q, Li Z, Cui W, Yu M, Ning X, Ramakrishna S, Long Y (2021) Robust graphene@PPS fibrous membrane for harsh environmental oil/water separation and all-weather cleanup of crude oil spill by joule heat and photothermal effect. Acs Appl Mater Inter 13:19377–19386. https://doi.org/10.1021/acsami.1c04066

Fotiou T, Triantis TM, Kaloudis T, O'Shea KE, Dionysiou DD, Hiskia A (2016) Assessment of the roles of reactive oxygen species in the UV and visible light photocatalytic degradation of cyanotoxins and water taste and odor compounds using C-TiO_2. Water Res 90:52–61. https://doi.org/10.1016/j.watres.2015.12.006

Gu J, Xiao P, Chen P, Zhang L, Wang H, Dai L, Song L, Huang Y, Zhang J, Chen T (2017) Functionalization of biodegradable PLA nonwoven fabric as superoleophilic and superhydrophobic material for efficient oil absorption and oil/water separation. Acs Appl Mater Inter 9:5968–5973. https://doi.org/10.1021/acsami.6b13547

Huo Q, Liu G, Sun H, Fu Y, Ning Y, Zhang B, Zhang X, Gao J, Miao J, Zhang X, Liu S (2021) CeO_2-modified MIL-101(Fe) for photocatalysis extraction oxidation desulfurization of model oil under visible light irradiation. Chem Eng J 422:130036. https://doi.org/10.1016/j.cej.2021.130036

Ibrahim I, Kaltzoglou A, Athanasekou C, Katsaros F, Devlin E, Kontos AG, Ioannidis N, Perraki M, Tsakiridis P, Sygellou L, Antoniadou M, Falaras P (2020) Magnetically separable TiO_2/$CoFe_2O_4$/Ag nanocomposites for the photocatalytic reduction of hexavalent chromium pollutant under UV and artificial solar light. Chem Eng J 381:122730. https://doi.org/10.1016/j.cej.2019.122730

Jiang J, Zhang Q, Zhan X, Chen F (2019) A multifunctional gelatin-based aerogel with superior pollutants adsorption, oil/water separation and photocatalytic properties. Chem Eng J 358:1539–1551. https://doi.org/10.1016/j.cej.2018.10.144

Jin K, Zhao Y, Fan Z, Wang H, Zhao H, Huang X, Hou K, Yao C, Xie K, Cai Z (2021) A facile and green route to fabricate fiber-reinforced membrane for removing oil from water and extracting water under slick oil. J Hazard Mater 416:125697. https://doi.org/10.1016/j.jhazmat.2021.125697

Karimi-Maleh H, Kumar BG, Rajendran S, Qin J, Vadivel S, Durgalakshmi D, Gracia F, Soto-Moscoso M, Orooji Y, Karimi F (2020) Tuning of metal oxides photocatalytic performance using Ag nanoparticles integration. J Mol Liq 314:113588. https://doi.org/10.1016/j.molliq.2020.113588

Lee Y, Kim S, Jeong SY, Seo S, Kim C, Yoon H, Jang HW, Lee S (2021) Surface-modified co-doped ZnO photoanode for photoelectrochemical oxidation of glycerol. Catal Today 359:43–49. https://doi.org/10.1016/j.cattod.2019.06.065

Lei Y, Tian Z, Sun H, Liu F, Zhu Z, Liang W, Li A (2021) Low-resistance thiophene-based conjugated microporous

polymer nanotube filters for efficient particulate matter capture and oil/water separation. Acs Appl Mater Inter 13:5823–5833. https://doi.org/10.1021/acsami.0c20484

Li F, Kong W, Zhao X, Pan Y (2020) Multifunctional TiO_2-based superoleophobic/superhydrophilic coating for oil-water separation and oil purification. Acs Appl Mater Inter 12:18074–18083. https://doi.org/10.1021/acsami.9b22625

Li T, Abdelhaleem A, Chu W, Xu W (2021) Efficient activation of oxone by pyrite for the degradation of propanil: Kinetics and degradation pathway. J Hazard Mater 403:123930. https://doi.org/10.1016/j.jhazmat.2020.123930

Lin D, Zeng X, Li H, Lai X, Wu T (2019) One-pot fabrication of superhydrophobic and flame-retardant coatings on cotton fabrics via sol-gel reaction. J Colloid Interf Sci 533:198–206. https://doi.org/10.1016/j.jcis.2018.08.060

Liu H, Yang L, Zhan Y, Lan J, Shang J, Zhou M, Lin S (2021a) A robust and antibacterial superhydrophobic cotton fabric with sunlight-driven self-cleaning performance for oil/water separation. Cellulose 28:1715–1729. https://doi.org/10.1007/s10570-020-03585-w

Liu HJ, Wang BJ, Chen M, Zhang H, Peng JB, Ding L, Wang WF (2021b) Simple synthesis of BiOAc/BiOBr heterojunction composites for the efficient photocatalytic removal of organic pollutants. Sep Purif Technol. https://doi.org/10.1016/j.seppur.2020.118286

Liu K, Jiang L (2011) Metallic surfaces with special wettability. Nanoscale 3:825–838. https://doi.org/10.1039/c0nr00642d

Ma W, Ding Y, Zhang M, Gao S, Li Y, Huang C, Fu G (2020a) Nature-inspired chemistry toward hierarchical superhydrophobic, antibacterial and biocompatible nanofibrous membranes for effective UV-shielding, self-cleaning and oil-water separation. J Hazard Mater. https://doi.org/10.1016/j.jhazmat.2019.121476

Ma W, Li Y, Zhang M, Gao S, Cui J, Huang C, Fu G (2020b) Biomimetic durable multifunctional self-cleaning nanofibrous membrane with outstanding oil/water separation, photodegradation of organic contaminants, and antibacterial performances. Acs Appl Mater Inter 12:34999–35010. https://doi.org/10.1021/acsami.0c09059

Nayak K, Kumar A, Das P, Tripathi BP (2021) Amphiphilic antifouling membranes by polydopamine mediated molecular grafting for water purification and oil/water separation. J Membr Sci 630:119306. https://doi.org/10.1016/j.memsci.2021.119306

Nong Y, Ren Y, Wang P, Zhou M, Yu Y, Yuan J, Xu B, Wang Q (2021) A facile strategy for the preparation of photothermal silk fibroin aerogels with antibacterial and oil-water separation abilities. J Colloid Interf Sci 603:518–529. https://doi.org/10.1016/j.jcis.2021.06.134

Pan B, Feng M, McDonald TJ, Manoli K, Wang C, Huang CH, Sharma VK (2020) Enhanced ferrate(VI) oxidation of micropollutants in water by carbonaceous materials: elucidating surface functionality. Chem Eng J 398:125607. https://doi.org/10.1016/j.cej.2020.125607

Pan ZH, Cao SJ, Li JF, Du ZP, Cheng FQ (2019) Anti-fouling TiO_2 nanowires membrane for oil/water separation: Synergetic effects of wettability and pore size. J Membr Sci 572:596–606. https://doi.org/10.1016/j.memsci.2018.11.056

Pérez-González M, Tomás SA (2021) Surface chemistry of TiO_2-ZnO thin films doped with Ag. Its role on the photocatalytic degradation of methylene blue. Catal Today 360:129–137. https://doi.org/10.1016/j.cattod.2019.08.009

Qu M, Liu Q, Yuan S, Yang X, Yang C, Li J, Liu L, Peng L, He J (2021a) Facile fabrication of TiO_2-functionalized material with tunable superwettability for continuous and controllable oil/water separation, emulsified oil purification, and hazardous organics photodegradation. Colloids Surf, A. https://doi.org/10.1016/j.colsurfa.2020.125942

Qu M, Pang Y, Li J, Wang R, He D, Luo Z, Shi F, Peng L, He J (2021) Eco-friendly superwettable functionalized-fabric with pH-bidirectional responsiveness for controllable oil-water and multi-organic components separation. Colloids Surf, A. https://doi.org/10.1016/j.colsurfa.2021b.126817

Su B, Tian Y, Jiang L (2016) Bioinspired interfaces with superwettability: from materials to chemistry. J Am Chem Soc 138:1727–1748. https://doi.org/10.1021/jacs.5b12728

Tang S, Chang X, Li M, Ge T, Niu S, Wang D, Jiang Y, Sun S (2021) Fabrication of calcium carbonate coated-stainless steel mesh for efficient oil-water separation via bacterially induced biomineralization technique. Chem Eng J 405:126597. https://doi.org/10.1016/j.cej.2020.126597

Ueda E, Levkin PA (2013) Emerging applications of superhydrophilic-superhydrophobic micropatterns. Adv Mater 25:1234–1247. https://doi.org/10.1002/adma.201204120

Wang M, Zhang M, Gao Q, Liu Y, Zhang M, Shen R, Zhang Y, Hu J, Wu G (2020) Tightly-coated and easily recyclable Ag@AgBr-cotton hybrid photocatalyst for organic dye degradation under visible light. Cellulose 27:10047–10060. https://doi.org/10.1007/s10570-020-03453-7

Wang Y, Liu Z, Wei X, Liu K, Wang J, Hu J, Lin J (2021) An integrated strategy for achieving oil-in-water separation, removal, and anti-oil/dye/bacteria-fouling. Chem Eng J 413:127493. https://doi.org/10.1016/j.cej.2020.127493

Wei C, Dai F, Lin L, An Z, He Y, Chen X, Chen L, Zhao Y (2018) Simplified and robust adhesive-free superhydrophobic SiO_2-decorated PVDF membranes for efficient oil/water separation. J Membr Sci 555:220–228. https://doi.org/10.1016/j.memsci.2018.03.058

Xie X, Li S, Wang X, Huang J, Chen Z, Cai W, Lai Y (2021) An effective and low-consumption foam finishing strategy for robust functional fabrics with on-demand special wettability. Chem Eng J 426:131245. https://doi.org/10.1016/j.cej.2021.131245

Xu C, Yang F, Deng B, Che S, Yang W, Zhang G, Sun Y, Li Y (2021) RGO-wrapped Ti_3C_2/TiO_2 nanowires as a highly efficient photocatalyst for simultaneous reduction of Cr(VI) and degradation of RhB under visible light irradiation. J Alloys Compd 874:159865. https://doi.org/10.1016/j.jallcom.2021.159865

Yan S, Li Y, Xie F, Wu J, Jia X, Yang J, Song H, Zhang Z (2020) Environmentally safe and porous MS@TiO_2@PPy monoliths with superior visible-light photocatalytic properties for rapid oil-water separation and water purification. ACS Sustain Chem Eng 8:5347–5359. https://doi.org/10.1021/acssuschemeng.0c00360

Yang C, Wang P, Li J, Wang Q, Xu P, You S, Zheng Q, Zhang G (2021) Photocatalytic PVDF ultrafiltration membrane

blended with visible-light responsive Fe(III)-TiO_2 catalyst: Degradation kinetics, catalytic performance and reusability. Chem Eng J 417:129340. https://doi.org/10.1016/j.cej.2021.129340

Yang J, Wang H, Tao Z, Liu X, Wang Z, Yue R, Cui Z (2019) 3D superhydrophobic sponge with a novel compression strategy for effective water-in-oil emulsion separation and its separation mechanism. Chem Eng J 359:149–158. https://doi.org/10.1016/j.cej.2018.11.125

Yang Y, Guo Z, Huang W, Zhang S, Huang J, Yang H, Zhou Y, Xu W, Gu S (2020) Fabrication of multifunctional textiles with durable antibacterial property and efficient oil-water separation via in situ growth of zeolitic imidazolate framework-8 (ZIF-8) on cotton fabric. Appl Surf Sci https://doi.org/10.1016/j.apsusc.2019.144079

Yu T, Halouane F, Mathias D, Barras A, Wang Z, Lv A, Lu S, Xu W, Meziane D, Tiercelin N, Szunerits S, Boukherroub R (2020) Preparation of magnetic, superhydrophobic/superoleophilic polyurethane sponge: Separation of oil/water mixture and demulsification. Chem Eng J. https://doi.org/10.1016/j.cej.2019.123339

Yu X, Huang J, Zhao J, Liu S, Xiang D, Tang Y, Li J, Guo Q, Ma X, Zhao J (2021) Efficient visible light photocatalytic antibiotic elimination performance induced by nanostructured Ag/AgCl@Ti^{3+}-TiO_2 mesocrystals. Chem Eng J 403:126359. https://doi.org/10.1016/j.cej.2020.126359

Zhan Y, He S, Hu J, Zhao S, Zeng G, Zhou M, Zhang G, Sengupta A (2020a) Robust super-hydrophobic/super-oleophilic sandwich-like UIO-66-F4@rGO composites for efficient and multitasking oil/water separation applications. J Hazard Mater 388:121752. https://doi.org/10.1016/j.jhazmat.2019.121752

Zhan Y, He S, Hu J, Zhao S, Zeng G, Zhou M, Zhang G, Sengupta A (2020b) Robust super-hydrophobic/super-oleophilic sandwich-like UIO-66-F-4@rGO composites for efficient and multitasking oil/water separation applications. J Hazard Mater. https://doi.org/10.1016/j.jhazmat.2019.121752

Zhang M, Cui J, Lu T, Tang G, Wu S, Ma W, Huang C (2021) Robust, functionalized reduced graphene-based nanofibrous membrane for contaminated water purification. Chem Eng J 404:126347. https://doi.org/10.1016/j.cej.2020.126347

Zhao XX, Guan JR, Li JZ, Li X, Wang HQ, Huo PW, Yan YS (2021) CeO_2/3D g-C_3N_4 heterojunction deposited with Pt cocatalyst for enhanced photocatalytic CO_2 reduction. Appl Surf Sci .https://doi.org/10.1016/j.apsusc.2020.147891

Zheng XG, Fu WD, Kang FY, Peng H, Wen J (2018) Enhanced photo-Fenton degradation of tetracycline using TiO_2-coated alpha-Fe_2O_3 core-shell heterojunction. J Ind Eng Chem 68:14–23. https://doi.org/10.1016/j.jiec.2018.07.024

Zhou Y, Cai T, Liu S, Liu Y, Chen H, Li Z, Du J, Lei Z, Peng H (2021) N-doped magnetic three-dimensional carbon microspheres@TiO_2 with a porous architecture for enhanced degradation of tetracycline and methyl orange via adsorption/photocatalysis synergy. Chem Eng J 411:128615. https://doi.org/10.1016/j.cej.2021.128615